Crystal structure and enhanced electromechanical properties of Aurivillius ferroelectric ceramics, $Bi_4Ti_{3-x}(Mg_{1/3}Nb_{2/3})_xO_{12}$

Changbai Long,[*] Huiqing Fan,[*] Mengmeng Li, Guangzhi Dong and Qiang Li

State Key Laboratory of Solidification Processing, School of Materials Science and Engineering, Northwestern Polytechnical University, Xi'an 710072, People's Republic of China

The effect of Mg^{2+}/Nb^{5+} co-substitution at the B-site on the structures and electrical properties of modified Aurivillius ceramics, $Bi_4Ti_{3-x}(Mg_{1/3}Nb_{2/3})_xO_{12}$, was investigated. Rietveld refinement suggested that $Bi_4Ti_{3-x}(Mg_{1/3}Nb_{2/3})_xO_{12}$ crystallized in the orthorhombic space group $B2cb$ at room temperature. A high remnant polarization of 15.5 μC cm^{-2}, a large field-induced strain of 0.068% and a high piezoelectric activity of 30 pC N^{-1} were observed in $Bi_4Ti_{2.95}(Mg_{1/3}Nb_{2/3})_{0.05}O_{12}$, with a Curie point of 685 °C, due to an enhancement in structural distortion and a reduction in leakage current.
© 2013 Acta Materialia Inc. Published by Elsevier Ltd. All rights reserved.

Keywords: $Bi_4Ti_{3-x}(Mg_{1/3}Nb_{2/3})_xO_{12}$; Aurivillius ferroelectric ceramics; Piezoelectricity; Rietveld refinement; Leakage current

Aurivillius ferroelectrics (bismuth layer structure ferroelectrics, BLSFs) are thought to be promising candidates for nonvolatile ferroelectric random access memories and high-temperature piezoelectric transducers, due to their excellent fatigue-resistant properties and high Curie point (T_c), as well as their high-temperature stability [1–5]. The structure of BLSFs can be described as the intergrowth of $(Bi_2O_2)^{2+}$ slabs and $(A_{n-1}B_nO_{3n+1})^{2-}$ units, where n ($n = 1$–6) is the number of octahedral layers in the perovskite layers. Among these materials, $Bi_4Ti_3O_{12}$ (BiT) has attracted much attention because of its strong ferroelectric polarization and high T_c of 675 °C [5–8]. The polar axis of BiT single crystals is angled ~4.5° from the a–b plane. Its spontaneous polarization (P_s) values along the a and c axis are about 50 and 4 μC cm^{-2}, respectively [7]. However, despite prodigious efforts to integrate BiT into device applications, a remnant polarization (P_r) of BiT thin films and ceramics of only 7.5 μC cm^{-2} [9,10] was achieved, because of their high leakage current and the domain pinning caused by defects. Extensive studies have revealed that the oxygen vacancies ($V_O^{··}$) associated with bismuth vacancies (V_{Bi}''') in the perovskite layers are responsible for the domain-wall pinning,

polarization fatigue and high electrical leakage of BiT materials [11,12]. In addition the, large coercive field (E_c) and the high electrical conductivity originating from the coexistent Ti^{3+} and Ti^{4+} ions resulted in a low piezoelectric activity ($d_{33} \leqslant 8$ pC N^{-1}) of BiT, owing to a very low poling field [5,13,14]. Lanthanoid cation isovalent substitution for the A-site Bi^{3+} has been found to be an effective way to reduce bismuth vacancies and stabilize oxygen ions in the perovskite layers [2,15,16]. $Bi_{3.25}La_{0.75}Ti_3O_{12}$ (BLT) films exhibited high ferroelectric polarization ($P_r = 12$ μC cm^{-2}) and excellent fatigue-free characteristics [2]. On the other hand, B-site donor substitution with high valence cations (V^{5+}, W^{6+}, Nb^{5+}, Ta^{5+} and mixture of them, etc.) was also proposed [17,18]. For example, $Bi_4Ti_{2.98}Nb_{0.01}Ta_{0.01}O_{12}$ ceramics had a high d_{33} of 26 pC N^{-2}, due to the distortion of oxygen octahedra and the reduction in the concentration of oxygen vacancies.

In the present work, we selected $(Mg_{1/3}Nb_{2/3})$ to isovalently substitute the B-site Nb to improve the piezoelectric and ferroelectric properties of BiT-based materials. In order to compensate the bismuth vacancies (V_{Bi}''') and reduce the concentration of oxygen vacancies ($V_O^{··}$) caused by bismuth volatilization, excess Bi_2O_3 (2 wt.%) was introduced. $Bi_4Ti_{3-x}(Mg_{1/3}Nb_{2/3})_xO_{12}$ ceramics (BiT–(MgNb)x, $x = 0.05$ and 0.1) were prepared by using a solid-state reaction process. BiT- and 0.75La-substituted BLT ceramics were also prepared

[*] Corresponding authors. Tel.: +86 29 88494463; fax: +86 29 88492642; e-mail addresses: longchangbai@126.com; hqfan3@163.com

for comparison. The structures, leakage electrical currents, ferroelectric properties and electromechanical properties of the ceramics were studied in detail.

Stoichiometric quantities of starting materials (Bi_2O_3 (99.5%), TiO_2 (99.99%), MgO (99.99%), Nb_2O_5 (99.99%), La_2O_3 (99.99%)) were mixed using a ball-milling method in ethanol for 24 h. The mixtures were dried and then calcined at 800 °C for 4 h. The calcined powders were remilled in ethanol for 24 h, dried, ground and cold isostatically pressed into pellets at 300 MPa. The pressed pellets were then sintered at 1000–1030 °C for 2 h. Excess Bi_2O_3 (2 wt.%) was used. Powder X-ray diffraction (XRD) data were collected using an automated diffractometer (X'Pert PRO MPD, Philips, Eindhoven, the Netherlands) with a nickel filter (Cu K_α radiation) at room temperature. Surface morphologies of the ceramics were revealed by scanning electron microscopy (SEM; JSM-5610, JEOL, Tokyo, Japan). The temperature dependences of the dielectric properties of all samples were measured using an LCR meter (4284A, Agilent, CA, USA). Ferroelectric properties, electrostriction properties and leakage currents of the samples were measured using a ferroelectric analyzer (TF-2000, Aix ACCT, Aachen, Germany). After 90–100 kV cm^{-1} DC field poling in silicone oil for 20 min at 120 °C, d_{33} values of the BiT–(MgNb)0.05 and BiT–(MgNb)0.1 samples were measured at room temperature using a piezo-d_{33} meter (ZJ-3B, Institute of Acoustics, Chinese Academic of Science, Beijing, PR China).

XRD patterns of all samples are shown in Figure 1. No second phase is found for all samples, which means that Mg^{2+}/Nb^{5+} and La^{3+} were incorporated into the layered perovskite structure. According to the inset of Figure 1a, plate-like morphologies were observed for BiT and BiT–(MgNb)0.1 ceramics, which is typical characteristic of Aurivillius ceramics due to the anisotropic nature of crystal structure. It is clear that the $(Mg_{1/3}Nb_{2/3})$ substitution caused a decrease in grain size, which could be attributed to the reduction of crystal growth kinetics resulting from an enhancement of the structure distortion. In order to further characterize the structure of the samples, powder diffraction Rietveld refinement for BiT–(MgNb)0.05 was carried out using the GSAS-EXPGUI program. The XRD data were collected in the 2θ range of 10°–130° with a step size of 0.02° and a step time of 10 s, at room temperature. The crystal structure of BiT was first proposed to be orthorhombic symmetry ($B1bc$, transformed from $B2cb$) by Dorrian et al. [19], and can be also refined in the orthorhombic space group $B2cb$ [20]. However, Rae et al. suggested a monoclinic structure, $B1a1$ [21], which can be regarded as orthorombic because the β angle is 90.01°. Therefore, orthorhombic symmetry was selected for the refinement of BiT–(MgNb)0.05, and the BiT coordinates in space group $B2cb$ (ICSD no. 240210) were used as an initial model. From inspection of Figure 1b, the refined profile fits well with the experimental data, with reliability factors, R_{wp}, R_p and reduced χ^2 values of 8.73%, 6.49% and 1.576, respectively. The refined structure parameters are listed in Table S1 (Supplementary Material), and the lattice parameters of the BiT–(MgNb)0.05 are $a = 5.45214(9)$ Å, $b = 5.41439(9)$ Å and $c = 32.86097(27)$ Å. On the basis of the refined results, the BiT–(MgNb)0.05 crystal structures viewed along the [010] and [100] directions at room temperature are depicted in the inset of Figure 1b. In addition, P_s of the BiT–(MgNb)0.05 can be calculated from the atomic displacements along the a axis by using Shimakawa's model [22]. The calculated P_s of the BiT–(MgNb)0.05 is 38.5 μC cm^{-2} which is higher than that of BiT, 35.7 μC cm^{-2} (Fig. S1, Supplementary Material).

Table S2 (Supplementary Material) lists the lattice parameters (a, b and c) of all samples (see also Fig. 2a). Clearly, B-site substitution leads to an increase in a, b and c of the BiT–(MgNb)x samples, because both Mg^{2+} and Nb^{5+} (0.72 and 0.64 Å, respectively, 6 coordination number (CN)) are larger in size than Ti^{4+} (0.605 Å, 6 CN). Nevertheless, the BLT sample exhibits a sharp decrease in a as well as a slight increase in b and c, even though Bi^{3+} (12 CN, 1.38 Å) and La^{3+} (12 CN, 1.36 Å) have similar radii. This can be attributed to the replacement of the polar Bi^{3+} with $6s^2$ lone-pair electrons by the non-polar La^{3+}. Figure 2b demonstrates the temperature dependence of dielectric permittivity and dielectric loss of all samples. T_c of BiT is 677 °C. The BiT–(MgNb)0.05 has a higher T_c of 685 °C due to the substitution of larger Mg^{2+}/Nb^{5+} at B-sites. However, further Mg^{2+}/Nb^{5+} substitution induces a slight decrease in T_c for BiT–(MgNb)0.1, which may be due to the contribution of space charge and ionic motion [17]. Relatively, the La^{3+} substitution results in a dramatic reduction in the phase temperature of BLT ($\sim$380 °C). This is closely related to the obvious relaxation of the orthorhombic distortion of BLT, defined as $2(a-b)/(a+b)$, which decreases from 7.05×10^{-3} (BiT) to 1.19×10^{-3}. Additionally, the BiT and BiT–(MgNb)x
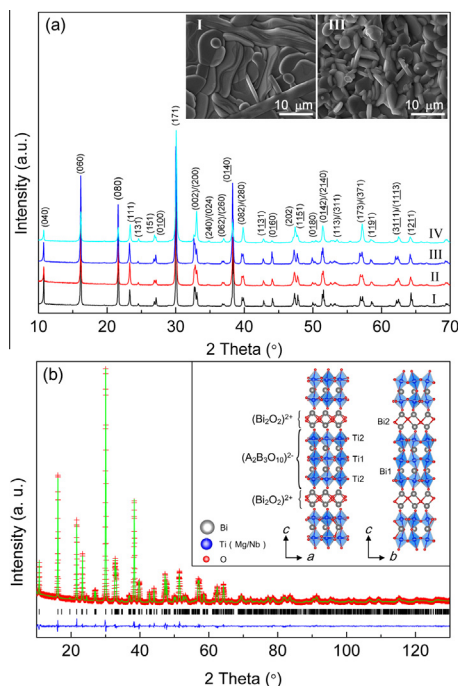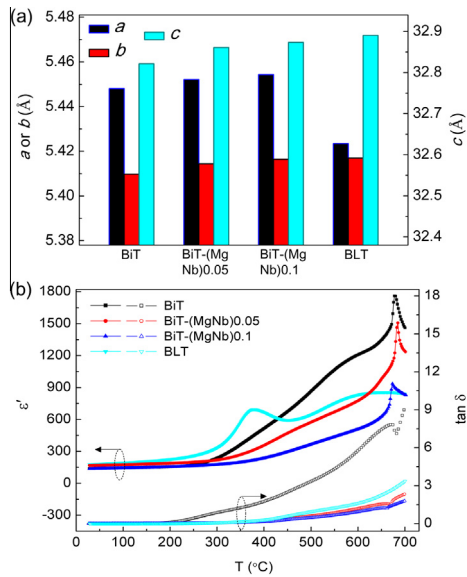

Fig. 1. (a) Powder XRD patterns of (I) BiT, (II) BiT–(MgNb)0.05, (III) BiT–(MgNb)0.1 and (IV) BLT ceramics, with insets showing surface SEM images of (I) BiT and (III) BiT–(MgNb)0.1 ceramics. (b) Rietveld refinement for BiT–(MgNb)0.05 at room temperature, viewed along the [010] and [100] directions for BiT–(MgNb)0.05 as an inset.

Fig. 2. (a) Lattice parameters a, b and c of all the ceramics. (b) Temperature dependence of the dielectric permittivity and dielectric loss of all ceramics at 100 k Hz.

samples have a loss peak just below T_c, and the height of the peaks of the BiT–(MgNb)x samples is reduced significantly due to the Mg^{2+}/Nb^{5+} substitution.
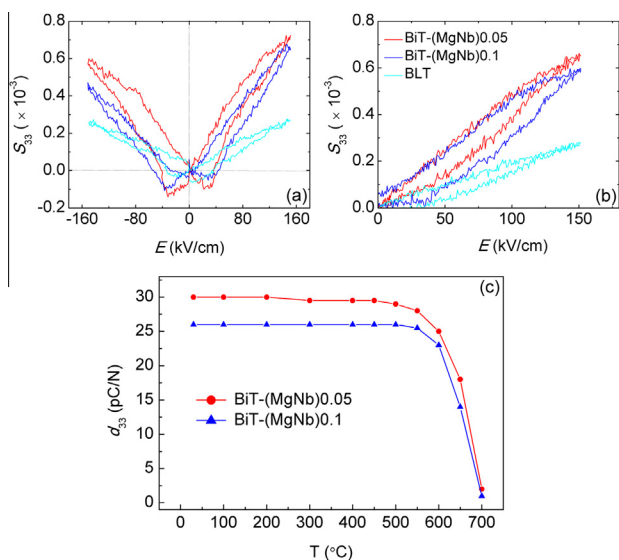
Ferroelectric hysteresis (P–E) loops of all samples are shown in Figure 3a. It is observed that pure BiT is a typical lossy dielectric and its P–E loop is dominated by high leakage current and high electrical conductivity [23]. With B-site Mg^{2+}/Nb^{5+} and A-site La^{3+} substitutions, standard P–E loops were observed, though a higher applied field is required. In addition, a significant enhancement in ferroelectric polarization is found for the modified samples. The BiT–(MgNb)0.05 has a P_r of 15.5 μC cm^{-2}, much higher than those of BiT (9.3 μC cm^{-2}) and BLT (11 μC cm^{-2}). The remarkable enhancement in ferroelectric polarization could be
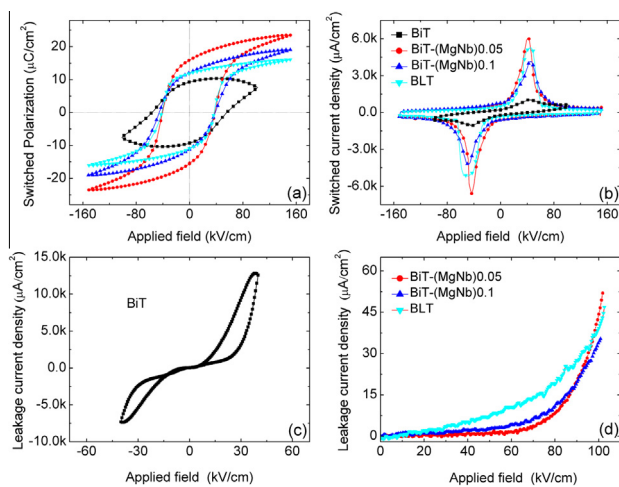
mainly due to the reduction of leakage current and electrical conductivity. Moreover, an increased P_s (38.5 μC cm^{-2}) with a local lattice distortion partly contributes to the increased P_r of the BiT–(MgNb)0.05. However, further Mg^{2+}/Nb^{5+} substitution induces an obvious decrease in the polarization of the BiT–(MgNb)0.1, which could be ascribed to a dimensional mismatch between perovskite and bismuth oxide layers due to the high concentration substitution. Figure 3b shows current density loops (J–E) of all samples, which are related to the switching of ferroelectric domains by an external field. Clearly, the BiT–(MgNb)x and BLT samples have intensive current density peaks for the switched domains, whereas weak peaks are observed for the pure BiT. This suggests that the polarization of BiT in the P–E loop cannot be attributed mainly to the reversal of the ferroelectric domains, but may be induced by high leakage current and strong conduction. DC field measurements confirm the high leakage current of pure BiT. Figure 3c reveals a typical leakage current–density loop of the BiT sample; the magnitude reaches $\sim$10^{-2} A cm^{-2} at low field (40 kV cm^{-1}). The high leakage current of the BiT ceramic is mainly caused by the instability of the oxidation state of the Ti ion and the high ion-jump conduction of Ti^{4+} $\leftrightarrow$ Ti^{3+} [13,17]. In comparison, the BiT–(MgNb)x ceramics have much lower leakage currents at higher fields (Fig. 3d), with current density values of $<$0.05 × 10^{-3} A cm^{-2} at 100 kV cm^{-1} field and 120 °C. The oxygen vacancies (V$_O^{\cdot\cdot}$) resulting from the bismuth volatilization are strongly attracted by the defect cations, Mg$_{Ti}''$. Therefore, defect dipoles, (Mg$_{Ti}''$–V$_O^{\cdot\cdot}$)$^\times$, might be formed in the BiT–(MgNb)x samples. This would reduce the concentration of oxygen vacancies neighboring Ti^{4+} ions, and thus inhibit the reduction of Ti^{4+} to Ti^{3+}. In addition, the enhanced lattice distortion caused by the substitution of the larger size Mg^{2+}/Nb^{5+} could hinder the migration of oxygen ions/vacancies under an external field to a certain degree. Therefore, a significant decrease in leakage current density is observed in the BiT–(MgNb)x samples. Notably, the leakage currents of the BiT–(MgNb)x samples are close to that of the La^{3+}-substituted BLT sample (Fig. 3d).

Commonly, Aurivillius materials exhibit lower field-induced strains than other ferroelectrics, e.g. PMN and Bi$_{0.5}$Na$_{0.5}$TiO$_3$, because of their two-dimensional orientation restriction of the reversal of spontaneous polarization and their large E_c. Figure 4a shows bipolar field-induced strains (S_{33}) of the BiT–(MgNb)x and BLT samples. Their unipolar strains (S_{33}) are also given in Fig. 4b, and the maxima of which are all close to those of bipolar strains. The BiT–(MgNb)0.05 and BiT–(MgNb)0.1 have relatively large S_{33}, about 0.068% and 0.059%, respectively, which are much larger than those ($\leqslant$0.04%) of the two-layer Aurivillius ceramics in our previous works [24,25], and are comparable to that (0.06%) of K$_{0.5}$Bi$_{4.5}$Ti$_4$O$_{15}$ single crystals [26]. In comparison, a smaller strain, $\sim$0.028%, is observed in BLT. In addition, the piezoelectric constant (d_{33}^*) of the samples can be calculated directly from the slope of the strain vs. electric field curves. The d_{33}^* values of BiT–(MgNb)0.05, BiT–(MgNb)0.1 and BLT are 47.8, 43.7 and 18.7 pC N^{-1}, respectively. Furthermore, the

Fig. 3. (a) Switched polarizations and (b) the corresponding switched current densities of all ceramics measured at 120 °C and 10 Hz. (c,d) DC electric-field dependence of leakage current density of all ceramics at 120 °C.

Fig. 4. Electric-field-induced strain as a function of (a) bipolar and (b) unipolar electric field for the BiT–(MgNb)x and BLT ceramics at 120 °C and 10 Hz. (c) d_{33} of the poled BiT–(MgNb)x ceramics vs. temperature.

piezoelectric activities (d_{33}) of the samples can be measured after DC field poling. The d_{33} values of BiT–(MgNb)0.05 and BiT–(MgNb)0.1 are 30 and 26 pC N^{-1}, respectively, which are significantly higher than the reported d_{33} of pure BiT ($\leqslant$8 pC N^{-1}). The d_{33} value is much lower than $d_{33}{}^*$, because of the insufficient poling field (90–100 kV cm^{-1}). The effect of thermal depoling on the piezoelectric activities of the BiT–(MgNb)x samples is shown in Figure 4c. The d_{33} value was measured at room temperature after annealing for 2 h at each temperature (corresponding to the x-axis temperature). The two samples show no obvious drop in d_{33} when the annealing temperature is lower than 550 °C. After 550 °C thermal treatment, the BiT–(MgNb)0.05 and BiT–(MgNb)0.1 still have high d_{33} of 28 and 25.5 pC N^{-1}, respectively. This reveals that the piezoelectric activities of the BiT–(MgNb)x samples are very stable vs. temperature. When the annealing temperature is over 550 °C, the d_{33} of both samples decreases rapidly and becomes almost zero when the temperature is increased above T_c.

In summary, BiT–(MgNb)x ($x = 0.05$ and 0.1) ceramics have been synthesized via a solid-state reaction process. Rietveld refinement verified that BiT–(MgNb)x has an orthorhombic crystal structure, with space group $B2cb$, at room temperature. BiT–(MgNb)0.05 with a high T_c of 685 °C had a P_r of 15.5 μC cm^{-2}, a S_{33} of 0.068% and a d_{33} of 30 pC N^{-1}, because of the enhanced structural distortion and a reduction in electric conductivity. Additionally, d_{33} of the BiT–(MgNb)0.05 ceramics was very stable vs. temperature. These results suggest that the BiT-(MgNb)0.05 ceramics could be suitable for high-temperature piezoelectric applications.

[1] C.A. Paz de Araujo, J.D. Cuchiaro, L.D. McMillan, M.C. Scott, J.F. Scott, Nature 374 (1995) 627.
[2] B.H. Park, B.S. Kang, S.D. Bu, T.W. Noh, J. Lee, W. Jo, Nature 401 (1999) 682.
[3] H.X. Yan, H.T. Zhang, R. Ubic, M.J. Reece, J. Liu, Z. Shen, Z. Zhang, Adv. Mater. 17 (2005) 1261.
[4] Z.G. Gai, J.F. Wang, M.L. Zhao, W.B. Sun, S.Q. Sun, B.Q. Ming, Scr. Mater. 59 (2008) 115.
[5] H.X. Yan, H.T. Zhang, M.J. Reece, X.L. Dong, Appl. Phys. Lett. 87 (2005) 0829111.
[6] L.B. Kong, J. Ma, W. Zhu, O.K. Tan, Mater. Lett. 51 (2001) 108.
[7] S.E. Cummins, L.E. Cross, J. Appl. Phys. 39 (1968) 2268.
[8] H. Irie, M. Miyayama, T. Kudo, J. Appl. Phys. 90 (2001) 4089.
[9] P.C. Joshi, S.B. Krupanidhi, A. Mansingh, J. Appl. Phys. 72 (1992) 5517.
[10] X. Du, I.W. Chen, J. Am. Ceram. Soc. 81 (1998) 3253.
[11] B.H. Park, S.J. Hyun, S.D. Bu, T.W. Noh, J. Lee, H.D. Kim, T.H. Kim, W. Jo, Appl. Phys. Lett. 74 (1999) 1907.
[12] B.S. Kang, B.H. Park, S.D. Bu, S.H. Kang, T.W. Noh, Appl. Phys. Lett. 75 (1999) 2644.
[13] D.H. Kuo, K.C. Chiang, Thin Solid Films 516 (2008) 5985.
[14] J.G. Hou, Y.F. Qu, R. Vaish, D. Krsmanovic, R.V. Kumar, J. Am. Ceram. Soc. 94 (2011) 2523.
[15] H.C. Du, S. Wohlrab, S. Kaskel, J. Phys. Chem. C 111 (2007) 11095.
[16] U. Chon, K.B. Kim, H.M. Jang, G.C. Yi, Appl. Phys. Lett. 79 (2001) 3137.
[17] J.G. Hou, R.V. Kumar, Y.F. Qu, D. Krsmanovic, Scr. Mater. 61 (2009) 664.
[18] J.G. Hou, Qu, F.Y.R. Vaish, K.B.R. Varma, D. Krsmanovic, R.V. Kumar, J. Am. Ceram. Soc. 93 (2010) 1414.
[19] J.F. Dorrian, R.E. Newnham, D.K. Smith, Ferroelectrics 3 (1971) 17.
[20] C.H. Hervoches, P. Lightfoot, Chem. Mater. 11 (1999) 3359–3364.
[21] A.D. Rae, J.G. Thompson, R.L. Withers, A.C. Willis, Acta Crystallogr. B 46 (1990) 474.
[22] Y. Shimakawa, Y. Kubo, Y. Nakagawa, T. Kamiyama, H. Asano, F. Izumi, Appl. Phys. Lett. 74 (1999) 1904.
[23] J.F. Scott, J. Phys.: Condens. Matter 20 (2008) 0210011.
[24] C.B. Long, H.Q. Fan, Dalton Trans. 41 (2012) 11046.
[25] C.B. Long, H.Q. Fan, P.R. Ren, Inorg. Chem. 52 (2013) 5045.
[26] Y. Noguchi, M. Suzuki, Y. Kitanaka, S. Teranishi, M. Miyayama, Appl. Phys. Lett. 93 (2008) 0329041.